

## Dopamine as A Robust Anchor to Immobilize Functional Molecules on the Iron Oxide Shell of Magnetic Nanoparticles

Chenjie Xu,<sup>†</sup> Keming Xu,<sup>†,§</sup> Hongwei Gu,<sup>†</sup> Rongkun Zheng,<sup>‡</sup> Hui Liu,<sup>‡</sup> Xixiang Zhang,<sup>‡</sup> Zhihong Guo,<sup>†</sup> and Bing Xu<sup>\*,†,§</sup>

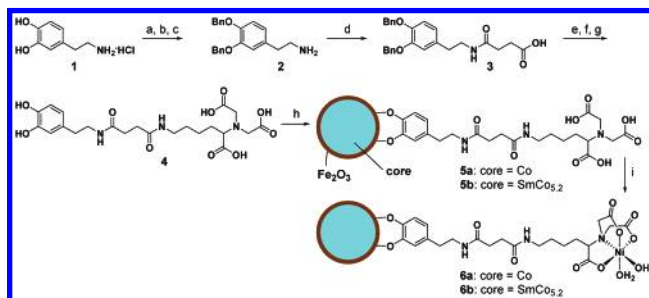
Department of Chemistry, Department of Physics, and Bioengineering Program, The Hong Kong University of Science and Technology, Clear Water Bay, Hong Kong, China

Received June 14, 2004; E-mail: chbingxu@ust.hk

This communication describes a general strategy that uses dopamine (DA) as a stable anchor to present functional molecules on the surface of iron oxide nanostructures. The successful synthesis of monodispersed magnetic nanoparticles,<sup>1</sup> particularly iron oxide nanoparticles<sup>2</sup> or core/shell nanostructures comprising iron oxides shells,<sup>3</sup> promises broad applications of magnetic nanoparticles in biomedicine and biology due to the inherent biocompatibility of iron oxide.<sup>4</sup> These applications, however, usually require designated molecules to be immobilized on the surfaces of the magnetic nanoparticles. Although thiolated organic molecules serve as excellent anchors to link the functional molecules on the magnetic nanoparticles whose surfaces consist of noble metals,<sup>5</sup> no demonstration shows that a small molecule acts as a versatile and robust anchor on a nanoparticle whose surface comprises iron oxide. Therefore, several alternatives have been developed to modify magnetic nanoparticles that consist of iron oxide—for example, coating iron oxide with Au, polymers, and silica.<sup>6</sup> These approaches, however, still have drawbacks such as low magnetic moments, low specificity, or poor tunability. Here we report an easy method that employs DA as a robust anchor to immobilize the functional molecules on the iron oxide shells of magnetic nanoparticles and the use of nitrilotriacetic acid (NTA) as the functional molecule for protein separation to demonstrate robustness and specificity of nanostructures created by this method.

We choose DA as the anchor to connect NTA to the iron oxide shell of the magnetic nanoparticles because the spectroscopic study by Rajh<sup>7</sup> suggested that bidentate enediol ligands such as DA convert the under-coordinated Fe surface sites back to a bulk-like lattice structure with an octahedral geometry for oxygen-coordinated iron, which may result in tight binding of DA to iron oxide. In addition, Langmuir isotherms indicate that the desorption of DA from metal oxide nanoparticles (e.g., TiO<sub>2</sub>) is less favorable than adsorption.<sup>8</sup> Thus, we created a system with an M/Fe<sub>2</sub>O<sub>3</sub>-DA-NTA (M = Co or SmCo<sub>5,2</sub>) nanostructure (**5**) and tested its stability and specificity. Upon chelation to Ni<sup>2+</sup>, this M/Fe<sub>2</sub>O<sub>3</sub>-DA-NTA-Ni<sup>2+</sup> system (**6**) separates histidine-tagged proteins from a cell lysate with high efficiency and capacity. In addition, the specificity and efficiency of **6b** remain unaffected even after **6b** is boiled in a buffer solution. The simple synthetic route provided in this work also allows a large pool of functional molecules to be connected to iron oxide. Because of the increasing usage of iron oxide nanoparticles in biological research, the ease of linking other biomolecules to iron oxide surfaces through a versatile anchor, such as DA, should lead to useful applications of iron oxide-containing nanostructures in several areas, e.g., cell biology, biotechnology, and environment monitoring.

Scheme 1<sup>a</sup>



<sup>a</sup> Conditions: (a) NaOH, *tert*-butyl dicarbonate, dioxane, H<sub>2</sub>O, 24 hrs; (b) BnBr, K<sub>2</sub>CO<sub>3</sub>, DMF, rt, 24 h; (c) 10% CF<sub>3</sub>COOH, CH<sub>2</sub>Cl<sub>2</sub>, rt, 5 h; (d) succinic anhydride, pyridine, rt, 3 h; (e) NHS, DCC, DMAP, CHCl<sub>3</sub>, rt, 3 h; (f) NaHCO<sub>3</sub>, NTA, H<sub>2</sub>O, CH<sub>3</sub>CH<sub>2</sub>OOH, CHCl<sub>3</sub>, rt, 24 h; HCl; (g) Pd/C, CH<sub>3</sub>OH, H<sub>2</sub>; (h) hexane/water, sonication for 20 min; and (i) NiCl<sub>2</sub>·6H<sub>2</sub>O.

Scheme 1 illustrates the synthetic route for making the M/Fe<sub>2</sub>O<sub>3</sub>-DA-NTA agents. After protecting the hydroxyl groups of dopamine (**1**) with benzyl bromide, succinic acid anhydride reacts with **2** to yield **3**. *N*<sub>α</sub>,*N*<sub>α</sub>-bis(carboxymethyl)lysine reacts with **3** to give **4** after deprotecting the hydroxyl group. Co (or SmCo<sub>5,2</sub>)/Fe<sub>2</sub>O<sub>3</sub> nanoparticles<sup>9</sup> (in hexane phase) react with **4** (in aqueous solution) under vigorous stirring overnight or under sonication for 20 min to form Fe-O bonds that link **4** to the Fe<sub>2</sub>O<sub>3</sub> shell. After the reaction, the resulting product, **5**, becomes water soluble and is easily separated from the organic phase. Then, excess amounts of NiCl<sub>2</sub>·6H<sub>2</sub>O react with **5** in the aqueous phase. The removal of the unreacted Ni<sup>2+</sup> solution followed by washing the nanoparticles with Tris buffer solution yields **6**.

We used UV-vis, infrared, and time-of-flight second ion mass spectra (ToF-SIMS) to characterize the DA-NTA moieties on the surface of Fe<sub>2</sub>O<sub>3</sub>.<sup>10</sup> In addition to the absorptions originating from the nanoparticles, the presence of a small peak at 280 nm (originated from **4**) indicates that DA-NTA resides on the nanoparticle. The IR spectra of **5a** and **5b** both exhibit broad peaks around 3440 cm<sup>-1</sup> and strong sharp peaks centered at 1640 cm<sup>-1</sup>, which arise for carboxylic acid groups and amide groups, indicating the presence of DA-NTA on **5**. The ToF-SIMS spectrum of **5** not only displays the fragments of **4** (*m/e* = 497, 478), but also the fragment of iron-coordinated dihydroxybenzyl moiety (FeO<sub>2</sub>C<sub>7</sub>H<sub>5</sub><sup>+</sup>, *m/e* = 177), further proving that DA-NTA forms covalent bonds with the Fe<sub>2</sub>O<sub>3</sub> shell. We also estimated the numbers of DA-NTA conjugate linked to the core-shell magnetic nanoparticles by weight analysis. We found that on each Co/Fe<sub>2</sub>O<sub>3</sub> and SmCo<sub>5,2</sub>/Fe<sub>2</sub>O<sub>3</sub> nanoparticle, there average 27 and 50 DA-NTA molecules, respectively.<sup>10</sup> TEM (Figure 1) indicates that **5a** or **5b** exhibits well-defined core-shell nanostructures (similar to the as-prepared Co/Fe<sub>2</sub>O<sub>3</sub> or SmCo<sub>5,2</sub>/Fe<sub>2</sub>O<sub>3</sub> nanoparticles).

<sup>†</sup> Department of Chemistry.

<sup>‡</sup> Department of Physics.

<sup>§</sup> Bioengineering Program.

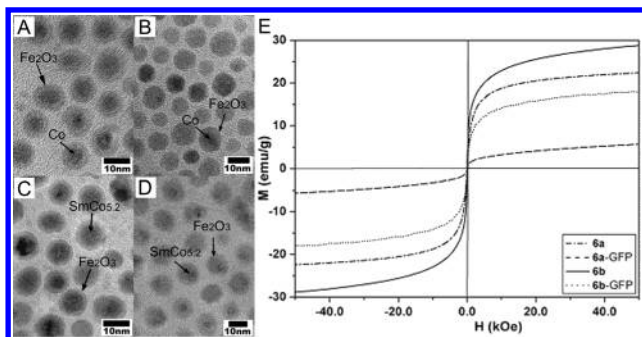


**Figure 1.** Transmission electron micrograph (TEM) images of (A) Co/Fe<sub>2</sub>O<sub>3</sub>, (B) **5a**, (C) SmCo<sub>5.2</sub>/Fe<sub>2</sub>O<sub>3</sub>, and (D) **5b**. (E) Magnetism of **6a**, **6a**-GFP, **6b**, and **6b**-GFP at the ambient conditions.<sup>10</sup>

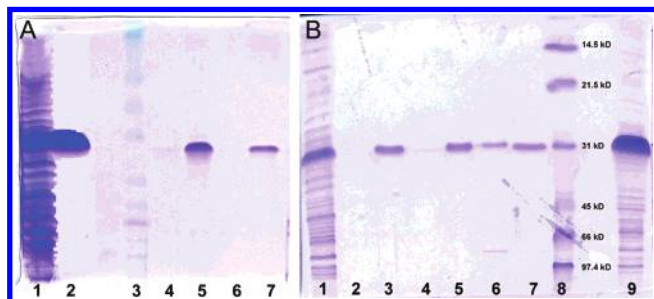


**Figure 2.** SDS/PAGE analysis of the purity of the proteins. (A) Cell lysate (lane 1), GFP standard (lane 2), the fractions from freshly made SmCo<sub>5.2</sub>/Fe<sub>2</sub>O<sub>3</sub>-NTA by washing with imidazole elutions (10 mM, lane 4; 500 mM, lane 5), fractions from the freshly made Co/Fe<sub>2</sub>O<sub>3</sub>-NTA using imidazole elutions (10 mM, lane 6; 500 mM, lane 7). (B) Cell lysate (lane 1), GFP standard (lane 2), the molecular weight marker (lane 8), the fractions washed from the freshly made **6b** (lanes 2 and 3), boiled **6b** (lanes 4 and 5), and the microbeads of the commercial HiTrap affinity column (lanes 6 and 9). The concentrations of imidazole are 10 mM (lanes 2, 4, and 6) and 500 mM (lanes 3, 5, 9). All imidazole elutions also contain 20 mM Na<sub>2</sub>HPO<sub>4</sub> and 0.5 M NaCl.

Magnetic measurements reveal the superparamagnetic behavior (no hysteretic behavior, Figure 1E) of **6a** and **6b** at 298 K before and after binding to the protein, respectively. Before binding to the protein (6xHis-GFP), the magnetization of **6a** is 14.5 emu/g at 3000 G, and the magnetization of **6b** is 18 emu/g at 3000 G. After binding to the proteins, the magnetization of **6a**-GFP is 2.2 emu/g at 3000G, while that of **6b**-GFP is 10.6 emu/g. Both magnetizations are sufficient to allow the magnetic nanoparticle-connected proteins to be attracted by a small magnet (with a surface field of ~4000 G).

The procedure and condition of using **6** to isolate proteins is similar to our previously reported process.<sup>11</sup> After washing away the physically absorbed proteins on **6** or the residual protein solutions by deionized water, we used 10 and 500 mM of imidazole elutions to sequentially wash the protein-bound nanoparticles. Figure 2A shows the imidazole elutions contain only the target protein (6xHis-GFP, lanes 4, 5, and 7). Since there is no other protein being washed off even by the low concentration (10 mM) imidazole elution (Figure 2A, lanes 4 and 6), **6** indeed enhances the specificity of NTA-Ni<sup>2+</sup> to bind with histidine-tagged proteins. Control experiment shows that the amount of GFP absorbed on **5** is almost negligible when there is no chelation of Ni<sup>2+</sup> ions with the NTA groups.<sup>10</sup> Both **6a** and **6b** can be regenerated and reused,<sup>10</sup> suggesting that the bonding between DA and iron oxide is stable at high salt concentration and the presence of sodium dodecyl sulfonate (the cell lysate contains 0.5 M NaCl, 20 mM Tris-Cl, and 2% SDS).

We tested the thermal stability of **6b** and compared its specificity with a commonly used commercial product for separating histidine-tagged proteins. As shown in Figure 2B, after being boiled in Tris buffer (pH = 7.9) for 20 min, the specificity and efficiency of **6b** remain unaffected—electrophoresis traces show that the fractions washed from the boiled **6b** contain only the histidine-tagged protein, the same as the fractions washed from the freshly made **6b**. Moreover, the specificity of **6b** for the histidine-tagged proteins is much higher than the commercial HiTrap affinity column that is based on microbeads: after the affinity column and **6b** were bathed with cell lysate and washed under the same conditions, the fraction washed from the affinity column contains many other proteins, while the fractions from **6b** contain only the histidine-tagged protein. In conclusion, we have demonstrated for the first time that dopamine serves as a robust anchor on the surface of the iron oxide shell of a magnetic nanoparticle, and the resulting nanostructure exhibits high specificity for protein separation and exceptional stability to heating and high salt concentration. Our simple synthetic strategy should provide a useful way to link other bifunctional molecules to other metal oxide surfaces (e.g., TiO<sub>2</sub><sup>12</sup> and Fe<sub>3</sub>O<sub>4</sub>) that also have high affinity to DA<sup>7</sup> and offer new opportunities for the biological applications of metal oxide nanoparticles.

**Acknowledgment.** This work was partially supported by RGC (Hong Kong), HIA (HKUST), and a DuPont Young Faculty Grant (to B.X.).

**Supporting Information Available:** The details of the synthesis and characterization of **6** and the separation of histidine-tagged proteins of reused **6**. This material is available free of charge via the Internet at <http://pub.acs.org>.

## References

- (1) (a) Sun, S. H.; Murray, C. B.; Weller, D.; Folks, L.; Moser, A. *Science* **2000**, *287*, 1989. (b) Punter, V. F.; Zanchet, D.; Erdonmez, C. K.; Alivisatos, A. P. *J. Am. Chem. Soc.* **2002**, *124*, 12874. (c) Zhang, Z. J.; Wang, Z. L.; Chakoumakos, B. C.; Yin, J. S. *J. Am. Chem. Soc.* **1998**, *120*, 1800. (d) Weller, D.; Moser, A. *IEEE Trans. Magn.* **1999**, *35*, 4423. (e) Tripp, S. L.; Pusztay, S. V.; Ribbe, A. E.; Wei, A. *J. Am. Chem. Soc.* **2002**, *124*, 7914. (f) Sun, S. H.; Zeng, H.; Robinson, D. B.; Raoux, S.; Rice, P. M.; Wang, S. X.; Li, G. X. *J. Am. Chem. Soc.* **2004**, *126*, 273. (g) Sun, S. H.; Anders, S.; Hamann, H. F.; Thiele, J. U.; Baglin, J. E. E.; Thomson, T.; Fullerton, E. E.; Murray, C. B.; Terris, B. D. *J. Am. Chem. Soc.* **2002**, *124*, 2884. (h) Majetich, S. A.; Artman, J. O.; McHenry, M. E.; Nuhfer, N. T.; Staley, S. W. *Phys. Rev. B* **1993**, *48*, 16845. (i) Gu, H. W.; Zheng, R. K.; Zhang, X. X.; Xu, B. *J. Am. Chem. Soc.* **2004**, *126*, 5664. (j) Punter, V. F.; Krishnan, K. M.; Alivisatos, A. P. *Science* **2001**, *291*, 2115.
- (2) (a) Park, S. J.; Kim, S.; Lee, S.; Khim, Z. G.; Char, K.; Hyeon, T. *J. Am. Chem. Soc.* **2000**, *122*, 8581. (b) Hyeon, T. *Chem. Commun.* **2003**, 927.
- (3) (a) Decker, S.; Klabunde, K. J. *J. Am. Chem. Soc.* **1996**, *118*, 12465. (b) Zeng, H.; Li, J.; Wang, Z. L.; Liu, J. P.; Sun, S. H. *Nano Lett.* **2004**, *4*, 187.
- (4) (a) Perez, J. M.; O'Loughin, T.; Simeone, F. J.; Weissleder, R.; Josephson, L. *J. Am. Chem. Soc.* **2002**, *124*, 2856. (b) Dyal, A.; Loos, K.; Noto, M.; Chang, S. W.; Spagnoli, C.; Shafi, K. V. P. M.; Ulman, A.; Cowman, M.; Gross, R. A. *J. Am. Chem. Soc.* **2003**, *125*, 1684.
- (5) (a) Gu, H.; Ho, P.-L.; Tsang, K. W.; Wang, L.; Xu, B. *J. Am. Chem. Soc.* **2003**, *125*, 15702. (b) Gu, H. W.; Ho, P. L.; Tsang, K. W. T.; Yu, C. W.; Xu, B. *Chem. Commun.* **2003**, 1966.
- (6) (a) Lyon, J. L.; Fleming, D. A.; Stone, M. B.; Schiffer, P.; Williams, M. E. *Nano Lett.* **2004**, *4*, 719. (b) Zhang, Y.; Kohler, N.; Zhang, M. *Biomaterials* **2002**, *23*, 1553. (c) Lu, Y.; Yin, Y. D.; Mayers, B. T.; Xia, Y. N. *Nano Lett.* **2002**, *2*, 183.
- (7) Chen, L. X.; Liu, T.; Thurnauer, M. C.; Csencsits, R.; Rajh, T. *J. Phys. Chem. B* **2002**, *106*, 8539.
- (8) Rajh, T.; Chen, L. X.; Lukas, K.; Liu, T.; Thurnauer, M. C.; Tiede, D. M. *J. Phys. Chem. B* **2002**, *106*, 10543.
- (9) Gu, H. W.; Xu, B.; Rao, J. C.; Zheng, R. K.; Zhang, X. X.; Fung, K. K.; Wong, C. Y. C. *J. Appl. Phys.* **2003**, *93*, 7589.
- (10) Supporting Information.
- (11) Xu, C.; Xu, K.; Gu, H.; Zhong, X.; Guo, Z.; Zheng, R. K.; Zhang, X. X.; Xu, B. *J. Am. Chem. Soc.* **2004**, *126*, 3392.
- (12) Rajh, T.; Saponjic, Z.; Liu, J.; Dimitrijevic, N. M.; Scherer, N. F.; Vega-Arroyo, M.; Zapol, P.; Curtiss, L. A.; Thurnauer, M. C. *Nano Lett.* **2004**, *4*, 1017 and references therein.

JA0464802